

# GAPartNet: Cross-Category Domain-Generalizable Object Perception and Manipulation via Generalizable and Actionable Parts

Haoran Geng<sup>1,2\*</sup> Helin Xu<sup>3\*</sup> Chengyang Zhao<sup>1\*</sup>  
 Chao Xu<sup>4</sup> Li Yi<sup>3</sup> Siyuan Huang<sup>2</sup> He Wang<sup>1†</sup>  
<sup>\*†1</sup>Peking University <sup>2</sup>Beijing Institute for General Artificial Intelligence  
<sup>3</sup>Tsinghua University <sup>4</sup>University of California, Los Angeles

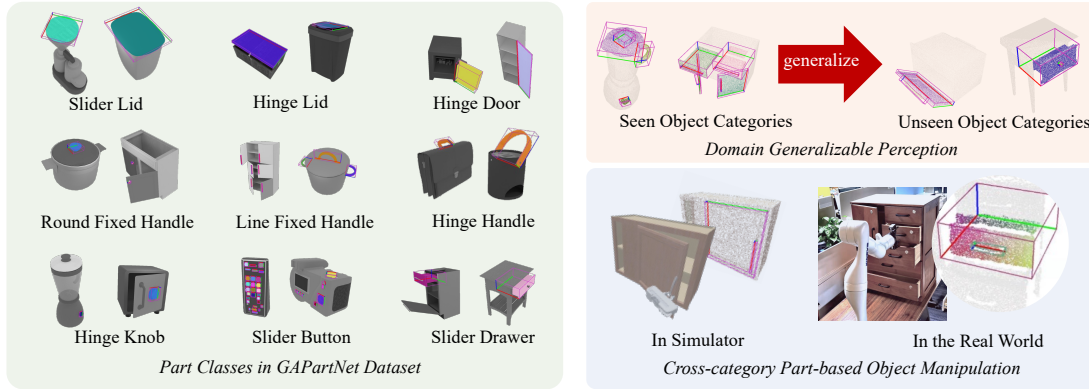


Figure 1. **Overview.** We propose to learn generalizable object perception and manipulation skills via **Generalizable and Actionable Parts**, and present **GAPartNet**, a large-scale interactive dataset with rich part annotations. We propose a domain generalization method for cross-category part segmentation and pose estimation. Our GAPart definition boosts cross-category robot manipulation and can transfer to real.

## Abstract

Perceiving and manipulating objects in a generalizable way has been actively studied by the computer vision and robotics communities, where cross-category generalizable manipulation skills are highly desired yet underexplored. In this work, we propose to learn such generalizable perception and manipulation via **Generalizable and Actionable Parts (GAParts)**. By identifying and defining 9 GAPart classes (*e.g.* buttons, handles, *etc.*), we show that our part-centric approach allows our method to learn object perception and manipulation skills from seen object categories and directly generalize to unseen categories. Following the GAPart definition, we construct a large-scale part-centric interactive dataset, GAPartNet, where rich, part-level annotations (semantics, poses) are provided for 1166 objects and 8489 part instances. Based on GAPartNet, we investigate three cross-category tasks: part segmentation, part pose estimation, and part-based object manipulation. Given the large domain gaps between seen and unseen object categories, we propose a

strong 3D segmentation method from the perspective of domain generalization by integrating adversarial learning techniques. Our method outperforms all existing methods by a large margin, no matter on seen or unseen categories. Furthermore, with part segmentation and pose estimation results, we leverage the GAPart pose definition to design part-based manipulation heuristics that can generalize well to unseen object categories in both simulation and real world. The dataset and code will be released.

## 1. Introduction

Generalizable object perception and manipulation are at the core of building intelligent and multi-functional robots. Recent efforts on generalizing the vision have been devoted to category-level object perception that deals with perceiving novel object instances from known object categories, including object detectors from RGB images [14, 20, 38], point clouds [5, 18], and category-level pose estimation works on rigid [4, 45] and articulated objects [24, 51]. On the front of generalizable manipulation, complex tasks that involve interacting with articulated objects have also been

\*Equal contribution with the order determined by rolling dice.

†Corresponding author.

proposed in a category-level fashion, as in the recent challenge on learning category-level manipulation skills [33]. Additionally, to boost robot perception and manipulation with indoor objects, researchers have already proposed several datasets [32, 49, 53, 57, 59] with part segmentation and motion annotations, and works have been devoted to part segmentation [32, 59] and articulation estimation [24].

However, these works all approach the object perception and manipulation problems in an intra-category manner, while humans can well perceive and interact with instances from unseen object categories based on prior knowledge of functional parts such as buttons, handles, lids, etc. In fact, parts from the same classes have fewer variations in their shapes and the ways that we manipulate them, compared to objects from the same categories. We thus argue that part classes are more elementary and fundamental compared to object categories, and generalizable visual perception and manipulation tasks should be conducted at part-level.

Then, what defines a part class? Although there is no single answer, we propose to identify part classes that are generalizable in both recognition and manipulation. After careful thoughts and expert designs, we propose the concept of *Generalizable and Actionable Part (GAPart)* classes. Parts from the same GAPart class share similar shapes which allows generalizable visual recognition; parts from the same GAPart class have aligned actionability and can be interacted with in a similar way, which ensures minimal human effort when designing interaction guidance to achieve generalizable and robust manipulation policies.

Along with the GAPart definition, we present GAPartNet, a large-scale interactive part-centric dataset where we gather 1166 articulated objects from PartNet-Mobility dataset [53] and AKB-48 [27]. We put in great effort in identifying and annotating semantic labels to 8489 GAPart instances. Moreover, we systematically align and annotate the GAPart poses, which we believe serve as the bridge between visual perception and manipulation. Our class-level part pose definitions highly couple the part poses with how we want to interact with the parts. We show that this is highly desirable – once the part poses are known, we can easily manipulate the parts using simple heuristics.

Based on the proposed dataset, we further explore three cross-category tasks based on GAParts: part segmentation, part pose estimation, and part-based object manipulation, where we aim at recognizing and interacting with the parts from novel objects in both known categories and, moreover, unseen object categories. Note that different object categories may contain different kinds of GAParts and provide different contexts to the parts. Each object category thus forms a unique domain for perceiving and manipulating GAParts. Therefore, all three tasks demand domain-generalizable methods that can work on unseen object categories without seeing them during training, which is in na-

ture very challenging for existing vision and robotic algorithms.

In this work, we propose to use learning-based methods to deal with the perception tasks, and devise simple heuristics based on the perception outputs to achieve cross-category object manipulation. Inspired by the domain generalization literature [11, 12, 22], domain-generalizable perception usually requires domain-invariant representation learning. This is often achieved by leveraging domain adversarial learning, which introduces a domain classifier. During training, the classifier tries to distinguish the domains while the feature extractor tries to fool the classifier, which encourages domain-invariant feature learning. However, it is highly non-trivial to adopt adversarial learning in our domain-invariant feature learning, due to the following challenges. (1) *Handling huge variations in part contexts across different domains.* The context of a GAPart class can vary significantly across different object categories. For example, in training data, round handles usually sit on the top of lids for coffeemachine category, whereas for a test category, table, round handles often stand to the front face of the drawers. To robustly segment GAParts in objects from unseen object categories, we need the part features to be context-invariant. (2) *Handling huge variations in part sizes.* Parts from different GAPart classes may be in different sizes, e.g. a button is usually much smaller than a door. Given that our input is a point cloud, the variations in part size will result in huge variations in the number of points across different GAParts, which makes feature learning very challenging. (3) *Handling imbalanced part distribution and part-object relations.* Object parts in the real world are naturally distributed unevenly and a particular part class may appear with different frequencies throughout various object categories. For example, there can be more buttons than doors on a washing machine while the opposite is true in the case of a storage furniture. This imbalanced distribution also adds difficulties to the learning of domain-invariant features.

To tackle these challenges, we propose several important innovations to domain adversarial learning. To improve the context invariance, we propose a part-oriented feature query process that mainly focuses on the foreground parts and ignore the background. To accommodate diverse part sizes, we propose a multi-resolution domain adversarial training strategy. Finally, we employ the focal loss to handle the distribution imbalance.

Our algorithm significantly outperforms previous 3D instance segmentation methods and achieves 76.5% AP50 on seen object categories and 37.2% AP50 on unseen object categories.

To summarize, our main contributions are as follows:

1. We provide part and pose definitions to *GAParts* and present a large-scale interactive dataset *GAPartNet* with rich

and well-defined part annotations that will facilitate generalizable part perception and manipulation.

2. We, for the first time, propose a pipeline for domain-generalizable 3D part segmentation and pose estimation via learning domain-invariant features, significantly outperforming the baselines.

3. We provide a new solution to generalizable object manipulation by leveraging the concept of GAParts. Thanks to innate generalizability and actionability, minimal human effort is needed when designing interaction guidance to achieve generalizable and robust manipulation policies.

## 2. Related Work

### Instance Segmentation for Parts/Objects from Point Cloud Observations.

Large-scale datasets of 3D shapes are fundamental to 3D part segmentation works, *e.g.* ShapeNet (2 ~ 5 parts per object) [3, 57] and PartNet (15 parts per object on average) [32]. Based on such datasets, much progress has been made on unified architectures for point cloud learning [25, 36, 37, 50], specialized supervised segmentation networks [48, 58], shape abstraction and part discovery [30, 34, 55, 56], *etc.* However, these works all approach the object perception problems in an intra-category manner, which hinders models’ ability to generalize perception and manipulation skills to novel object categories. We instead propose a new dataset GAPartNet, and tackle the 3D part instance segmentation problem in a cross-category way.

### Domain Generalization.

Domain Generalization is proposed to tackle the domain shift problem and try to learn from multiple source domains to generalize to the unseen domains. Due to the lack of relative dataset and benchmarks, 3D domain generalization are highly underexplored. [28, 29] try to discover parts in a category-agnostic manner, which are different from our tasks. Nevertheless, some 2D domain generalization or even domain adaptation methods can provide us with insights [17]. There are mainly three types of methods in this area [47]. Data manipulation methods use data augmentation or data generation techniques while another kinds of methods trying to find the general learning strategies to promote the generalization ability (*e.g.* ensemble learning). Representation learning is popular and focusing on learning domain-invariant representation, in which, Domain Adversarial Neural Network (DANN) [11, 12, 22] is well-used. They introduce a domain classifier to distinguish the domains, then the feature extractor is encouraged to fool the discriminator and learn domain-invariant features. However these works mainly focus on tasks like 2D image classification, whose techniques are not suitable to be directly used in our 3D multi-stage part segmentation and pose estimation tasks. Our tasks need to tackle irregular point cloud representation and take into account the multi-stage, multi-part

situation of the task itself.

### Category-level Object Pose Estimation.

There are a lot of works such as [16, 21, 26, 35, 39, 44, 54] on pose estimation that require the CAD model known, *i.e.* Instance-level object pose estimation, which has strong limitation due to the CAD model requirement.

Category-level object pose estimation is a more challenging task that deals with 3D bounding boxes prediction, 6D pose estimation on the *category level*. There are previous works on single-frame category-level pose estimation such as NOCS [45], FS-Net [6], CASS [4, 46] and works on category-level tracking such as 9-PACK [43], CAPTRA [51].

Wang *et al.* [45] innovated the Normalized Object Coordinate Space (NOCS), a unified coordinate space inside which objects of the same category are normalized, canonicalized and share an identical orientation. CASS [4] learns a canonical latent shape space for certain object categories, while [40] leverages category shape prior and models shape deformation to handle intra-class shape variation. FS-Net [6] designed a fast shape-based network that extracts efficient category-level pose feature. [46] used a cascaded relation network to relate 2D, 3D and shape prior, and proposed a recurrent reconstruction network to make iterative improvement.

**Generalizable Object Manipulation.** On the front of object manipulation, Mu *et al.* proposes [33] a challenge on learning generalizable manipulation skills for articulated objects from known categories.

Beyond category-level manner, one important further power is to generalize the perception and manipulation to complex objects in novel object categories, which is ubiquitously requested in handling many tasks in our daily life. Although, for simple rigid objects, we have already seen robust and object-agnostic object grasping [2, 8, 19] and planar pushing [23, 60] algorithms, very few works have been devoted to interact with articulated objects that contain movable parts. Recently, Mo *et al.* [31] and Wu *et al.* [52] tackles this problem leveraging a low-level generalizability – they estimate per-pixel actionability (*e.g.* pushing, pulling) or motion trajectories on the object surface and shows that their trained network can generalize to unknown objects. The most related work to us is Gadre *et al.* [10] that proposes an interesting interactive perception pipeline that first learns to touch the object, watch its movement, and then segment the object into movable parts. However, this work doesn’t consider the consistent geometry and actionability patterns behind parts from the same class and can only deal with simple objects with up to three parts on the table surfaces, *e.g.* scissors, eyeglasses.

### 3. GPart Definition and GPartNet Dataset

#### 3.1. GPart Definition

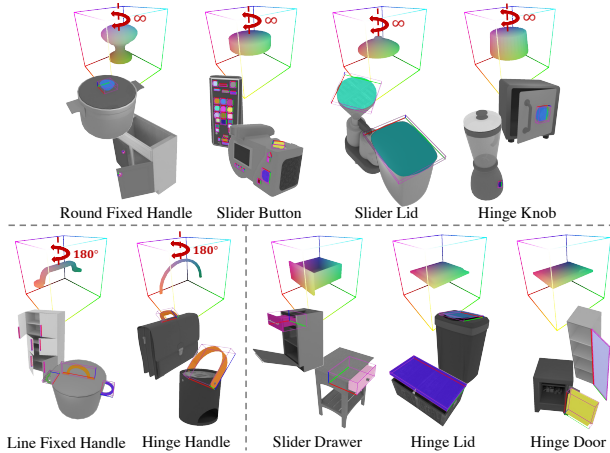


Figure 2. **GPart Classes.** Here we highlight the parts from 9 GPart classes along with their canonical part spaces. On the top, we show the four GPart classes that have continuous rotation symmetry along the z-axis, denoted with the red-dashed line and  $\infty$  remark; the bottom-left shows the two GPart classes that have  $180^\circ$  mirror symmetry along the z-axis; and the bottom-right shows the rest three asymmetric GPart classes.

Different from previous works, we give rigorous definitions to GPart classes which not only are Generalizable to visual recognition but also share similar Actionability, corresponding to the G and A in GPartNet. Our main purpose of such definitions is to bridge the perception and manipulation, to allow joint learning of both vision and interaction. Accordingly, we propose two principles to follow: **firstly, geometric similarity within part classes**, and **secondly, actionability alignment within part classes**.

**GPart Semantics.** Based on such principles, we identify 9 common GPart classes across 27 object categories: *line fixed handle*, *round fixed handle*, *hinge handle*, *hinge lid*, *slider lid*, *slider button*, *slider drawer*, *hinge door*, *hinge knob*.

Note that based on different actionability, handles are split into *fixed* handles and *hinge* handles, while lids are split into *hinge* lids and *slider* lids. We further identify *line* fixed handles and *round* fixed handles according to their difference in geometry.

**GPart Poses.** Following the previous works [24, 45], we define the canonicalized part position and orientation in Normalized Part Coordinate Space (NPCS). We illustrate our GPart pose definition in Figure 2. Note that some of the GPart classes have innate symmetry, which should be taken care of when using such pose definitions.

Based on the such rigorous and manipulation-oriented definitions, simple heuristics can be easily designed to

achieve generalizable part manipulation across different object categories, once we know their part classes as well as part poses. More details can be found in the appendix.

#### 3.2. GPartNet Dataset

Following the GPart definition, we construct a large-scale part-centric interactive dataset, GPartNet, with rich, part-level annotations for both perception and interaction tasks. The final GPartNet dataset has 9 GPart classes, and provides semantic labels and pose annotations for 8489 GPart instances on 1166 objects from 27 object categories. Our 3D object shapes come from two existing datasets, PartNet-Mobility [53] and AKB-48 [27]. We categorize the object shapes from these two sources and provide uniform annotation to 8489 part instances. On average, each object has 7.3 functional parts. Each GPart class can be seen on objects from more than three object categories, and each GPart class is found in 8.8 object categories on average, which corresponds to the G, *i.e.* Generalizability, in GPartNet.

Considering the realistic setting with plenty of novel objects, we further propose to split the object categories into seen and unseen categories to better study the generalizability. **Seen categories:** *Box, Bucket, Camera, CoffeeMachine, Dishwasher, Keyboard, Microwave, Printer, Remote, StorageFurniture, Toaster, Toilet, WashingMachine, Bucket(AKB-48), Box(AKB-48), Drawer(AKB-48), Trashcan(AKB-48)*. **Unseen categories:** *Door, KitchenPot, Laptop, Oven, Phone, Refrigerator, Safe, Suitcase, Table, TrashCan*.

Our split ensures that all GPart classes are seen within objects from seen categories, and also appear within unseen object categories. We suggest training a model to learn about the defined GPart classes on seen object categories, and testing its part understanding on unseen categories. This evaluates the performance of the model when it is facing a novel object for the first time, which is often the case in real-world indoor scenarios.

Table 1 and Figure 3 show the statistics and selected examples of GPartNet. More visualizations can be found in the appendix.

#### 3.3. Data Annotation

We direct systemic work to guarantee cross-category generalizable part semantics and pose annotations. After gathering the object shapes, we use the following pipeline to clean and annotate our data: (1) Fixing imperfect meshes and re-merging. We clean and fixing imperfect meshes of a percentage of original objects, and re-merge the meshes into new parts, to ensure that functional parts are segmented correctly. We manually fixed meshes of over 100 object instances and over 1000 functional part instances are newly merged. (2) Cross-category semantic label annotation. We



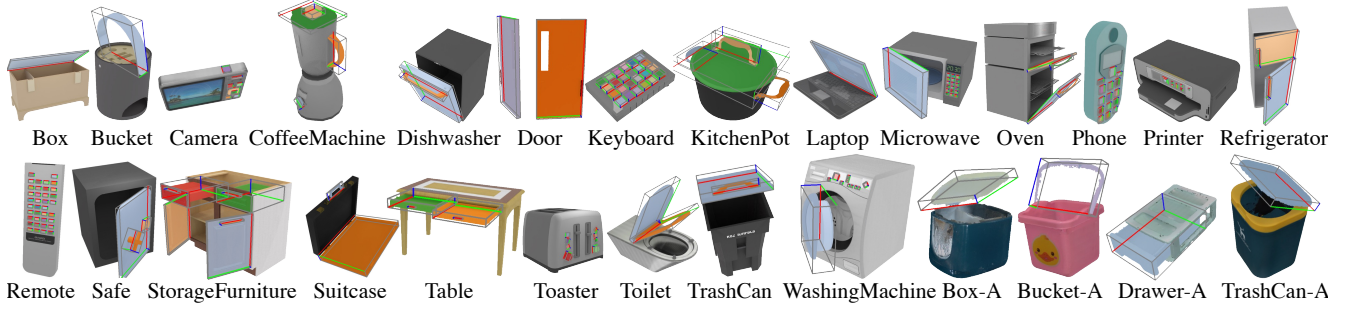


Figure 3. **GPartNet Objects.** Object assets collected from AKB-48 [27] end with '-A', while the others are from PartNet-Mobility [53].

	All	Bo	Bu	Ca	Co	Di	Do	Ke	Ki	La	Mi	Ov	Ph	Pr	Ref	Rem	Sa	St	Su	Ta	Toa	Toi	Tr	Wa	Bo-A	Bu-A	Dr-A	Tr-A
Object	1166	25	31	32	41	41	14	31	20	48	16	23	15	28	37	49	29	324	10	77	19	66	52	17	40	37	22	22
Ln.F.Hl.	922	2	-	-	10	28	2	-	40	-	5	29	-	-	43	-	1	667	-	60	-	-	35	-	-	-	-	-
Rd.F.Hl.	151	-	-	-	8	-	9	-	14	-	-	-	-	-	-	-	-	54	-	65	-	-	1	-	-	-	-	-
Hg.Hl.	78	-	31	-	-	-	-	-	-	-	-	-	-	-	-	-	-	-	10	-	-	-	-	-	-	37	-	-
Hg.Ld.	260	49	-	-	1	-	-	-	-	48	-	1	-	-	-	-	-	1	7	-	-	55	31	5	40	-	-	22
Sd.Ld.	89	-	-	1	19	-	-	-	20	-	-	-	-	-	-	-	-	-	-	-	44	5	-	-	-	-	-	-
Sd.Bn.	5526	-	-	208	140	5	-	2934	1	-	39	17	227	311	-	1433	89	-	2	-	24	15	-	81	-	-	-	-
Sd.Dw.	546	1	-	-	-	1	-	-	-	-	-	-	-	6	-	-	-	333	-	161	-	-	7	-	-	-	37	-
Hg.Dr.	678	-	-	-	-	41	18	-	-	-	16	28	-	-	60	-	29	433	-	24	-	-	15	14	-	-	-	-
Hg.Kb.	239	-	-	11	47	2	-	-	-	-	8	77	-	1	-	1	37	-	-	-	28	-	-	27	-	-	-	-

Table 1. **GPartNet Statistics.** We show how the GPart instances are distributed across all the object categories, where object categories titles are in the same order as in Figure 3, *e.g.* **Bo** = Box, **Bu** = Bucket, etc. The first row **Object** shows the object number for each object category. The following rows, *i.e.* line fixed handle, round fixed handle, hinge handle, hinge lid, slider lid, slider button, slider drawer, hinge door, hinge knob, show the number of GPart instances in each object category.

manually design heuristics to map each functional part in original assets to our GPart semantics. (3) Pose aligning. We build a whole pipeline as well as several manually designed rules to align and annotate the poses of all functional parts. More details can be found in the appendix.

## 4. Problem Formulation

Given the GPart definition and the proposed GPartNet dataset, we investigate the problems of cross-category generalizable object perception and manipulation.

**Perception.** The input to our system is the *partial* colored point cloud observation of the object  $P \in \mathbb{R}^{N \times 3}$ , where  $N$  denotes the number of points. Assume this object contains  $K$  GParts and the  $i$ -th part is with a class label  $p_i \in \{1, \dots, 9\}$ . Then the goal of our perception pipeline is as following: for each individual GPart, find its segmentation masks  $C'_i$  and recover its part pose, composed of a 3D rotation  $R_i \in \text{SO}(3)$ , 3D translation  $t_i \in \mathbb{R}^3$ , and a 3D size  $s_i \in \mathbb{R}$ .

Note that our perception tasks are carried out in a cross-category domain-generalizable fashion. We train the perception networks using objects from a set of seen object categories  $\{O_j^S\}_j$  (*i.e.*, seen domains  $\{D_j^S\}_j$ ) and we want to generalize them to unseen object categories  $\{O_j^U\}_j$  (*i.e.*,

unseen domains  $\{D_j^U\}_j$ ).

**Manipulation.** We need to develop a pose-based interaction policy  $\pi$  for generalizable part-based object manipulation. Given a single partial point cloud observation  $P \in \mathbb{R}^{N \times 3}$ , the robot needs to manipulate the target part using the previous understanding for the GParts, *e.g.* open a door on an object from a previous unseen object category.

## 5. Method

### 5.1. Domain-generalizable 3D Part Segmentation

**Architecture Overview.** Following the previous works [18, 42], our 3D part segmentation network leverages a Sparse U-Net [13] as the backbone to produce point-wise feature  $F$ , followed by a *Dual Set Grouping* model introduced by [18] for generating group proposals  $\mathcal{C}' = \{C'_1, C'_2, \dots, C'_{M'}\}$ . A total number of  $M$  proposals are then passed through and a *scoring module* that outputs the final segmentation masks  $\mathcal{C} = \{C_1, C_2, \dots, C_M\}$  after Non-Maximum Suppression (NMS). Most importantly, to enable domain-invariant feature extraction for part proposals and tackle the aforementioned challenges, we introduce a domain adversarial training strategy for 3D part segmentation to learn domain-invariant features.

**Domain-invariant GPart Feature Learning.** In-

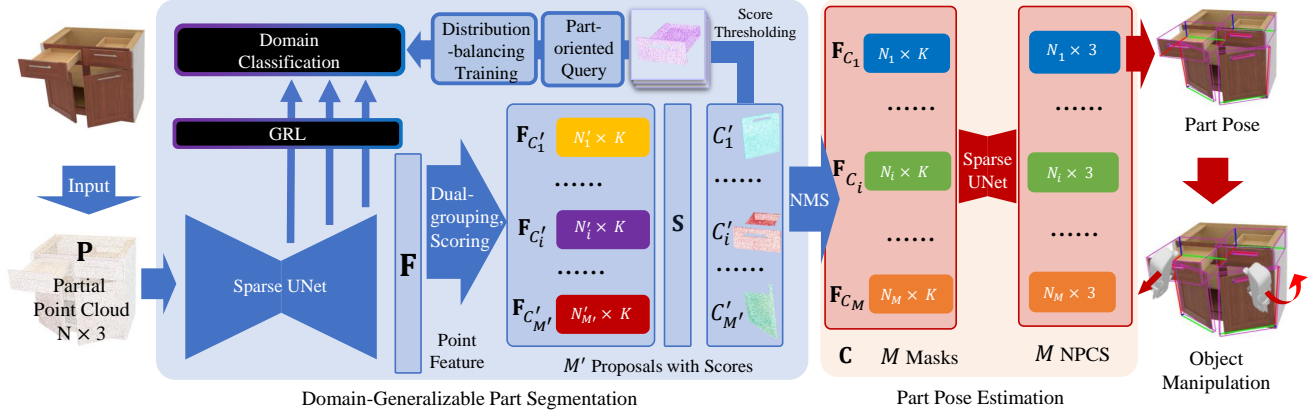


Figure 4. **An Overview of Our Domain-generalizable Part Segmentation and Pose Estimation Method.** We introduce part-oriented, multi-resolution and distribution-balancing domain adversarial learning method for the domain-invariant GAPart feature extraction, which tackles the challenges in our tasks and dataset, improving the generalization ability for part segmentation and pose estimation.

spired by [11, 12, 22], we introduce the domain classifier and gradient reverse layer (GRL) for domain adversarial training, as shown in Fig. 4. Specifically, the domain classifier takes the features as input and try to distinguish the different domains. The GRL makes the gradient of the classification negative and passes it back to the feature extractor, encouraging domain-invariant feature extraction during this adversarial training procedure.

Furthermore, to address the challenges mentioned in Sec. 4, we consider (1) how to process a feature map from the part segmentation pipeline to make GAPart feature domain-invariant, (2) where to place the domain classifier to better treat parts with different sizes, and (3) how to do domain adversarial training to tackle the distribution-imbalance problem. We thus design the following techniques to make our training strategy part-oriented, multi-resolution, and distribution-balancing.

1) *Part-oriented feature query (P)*. To better handle the huge variations in part contexts across different domains, the part features need to be context-invariant and have less domain-relative information. Thus, making the domain classifier  $\mathcal{D}$  part-oriented can better allow it to focus on the foreground (*i.e.*, the GAParts) rather than the background (*i.e.*, the rest of the object bodies), which often share little similarity across many categories. Our domain classifier takes as input foreground part proposals whose scores are greater than the threshold  $s_{thre}$ . We use  $P$  to indicate *Part-oriented feature query*, (*i.e.* for a proposal  $C'_i$ , we query its feature  $F_{C'_i}$  from the feature map  $F$  as input for domain classifier  $\mathcal{D}$ ) and the loss function is as follow:

$$\mathcal{L}_{P-adv}(F) = \frac{1}{M'_s} \sum_{i=1}^{M'} \mathbb{1}_{S(C'_i) > s_{thre}} \mathcal{L}_{cls}^{adv}(\mathcal{D}(F_{C'_i}), y_i^{cate}),$$

where  $M'$  indicates the number of proposals while  $M'_s$  is the number of proposals with score above the threshold  $s_{thes}$ .

$y_i^{cate}$  is the domain label (*i.e.* object category) for the proposal  $C'_i$ .

2) *Multi-resolution (M)*. Part instances come in significantly different sizes, *e.g.* a door can be an order of magnitude larger than a handle. We thus propose to extract the proposal features from different U-Net layers, each having different resolution, so that the size variance of GAParts is taken care of. In implementation, we choose three hidden layers from the U-Net decoder and query proposal features from the three feature maps respectively.

The multi-resolution, part-oriented adversarial loss  $\mathcal{L}_{PM-adv}$  can then be written as follows:

$$\mathcal{L}_{PM-adv} = \sum_{l=1}^3 w_l \mathcal{L}_{P-adv}(F^l),$$

where  $\mathcal{L}_{P-adv}(F^l)$  indicates the domain discrimination loss for features queried from the  $l^{th}$  layer and  $w_l$  is the corresponding weight for each discriminator.

3) *Distribution-balancing (D)*. As is often the case in the real world, part instances on different objects can be extremely imbalanced. We thus introduce a part-level domain discrimination focal loss for adversarial training in order to tackle the domain imbalance problem. During training, for a specific part class  $P$ , the loss weight  $w_{p_i}^{d_i}$  of different domains  $D$  are determined by the domain distribution. We modify the  $\mathcal{L}_{P-adv}$  as follows:

$$\mathcal{L}_{PD-adv}(F) = \frac{1}{M'_s} \sum_{i=1}^{M'} \mathbb{1}_{S(C'_i) > s_{thre}} w_{d_i}^{p_i} \mathcal{L}_{cls}^{adv}(\mathcal{D}(F_{C'_i}), y_i^{cate})$$

$$w_{d_i}^{p_i} = -\alpha_{d_i}^{p_i} (1 - a_{d_i}^{p_i})^\gamma,$$

where  $d_i$  and  $p_i$  are the domain category and part class for the  $i$ -th proposal  $C'_i$ , and  $w_{d_i}^{p_i}$  is the weight for the classification loss;  $\alpha_{d_i}^{p_i}$  is a hyper-parameter negatively correlated with the distribution of the number of parts in different domains in each part category while  $a_{d_i}^{p_i}$  is the mean accuracy

of the classification for the domain  $d_i$  in a certain part class  $p_i$  and  $\gamma$  is a hyper-parameter.

With the three techniques introduced, our proposed domain adversarial training method is part-oriented, multi-resolution and distribution-balancing, which better encourage the domain-invariant GPart feature learning. The final domain adversarial loss is  $\mathcal{L}_{\text{PMD-adv}} = \sum_{l=1}^3 w_l \mathcal{L}_{\text{PD-adv}}(F^l)$ , and the total loss for domain-generalizable part segmentation is as follows:

$$\mathcal{L}_{\text{seg}}^{\text{DG}} = \mathcal{L}_{\text{seg}} + \mathcal{L}_{\text{PMD-adv}},$$

where  $\mathcal{L}_{\text{seg}}$  is the part segmentation loss without domain adversarial training. Please refer to appendix for details.

## 5.2. Part Pose Estimation

With the domain-generalizable segmentation, we then introduce our part pose estimation method where we do domain-generalizable NPCS prediction and pose fitting. Considering the nature of our dataset, we are able to tackle the part pose symmetry and joint prediction problem, thanks to our part pose definition.

**NPCS Map Prediction and Pose Fitting.** For each predicted part segmentation  $C'_i$ , we query feature  $\mathbf{F}_{C'_i}$  from the feature map. Since the prediction of NPCS should be naturally independent of the context, color, etc. of the part, the feature in each of our proposal is more domain-invariant, thanks to our domain adversarial training. This significantly improves the generalization ability of pose estimation. We introduce our NPCS\_Net with a small Sparse U-Net and three Multilayer Perceptron (MLP) for point-wise NPCS coordinate regression. Followed with RANSAC [9] for outlier removal and Umeyama algorithm [41], we compute the 7-dimensional rigid transformation estimation problem and get the pose of the predicted part.

**Symmetry-aware Pose Estimation and Joint Prediction.** Since some part classes naturally have symmetries, we design an NPCS regression loss for each symmetry type that tolerates different symmetries for different part classes; please refer to the appendix for more details. We then follow our definition to simplify the joint prediction procedure. For each GPart class, the part pose definition contains a wealth of information, including the joint position and direction. This means given the part pose, we can directly get the joint position and direction and do not need an additional network for joint estimation as in previous works [24], thanks to our part pose definition. We describe our prediction process in more details and give examples in the appendix.

## 5.3. Interaction Policy

We introduce part-pose-based interaction policy, which provides with the community a novel approach to robotic manipulation and interaction tasks. With the proposed part

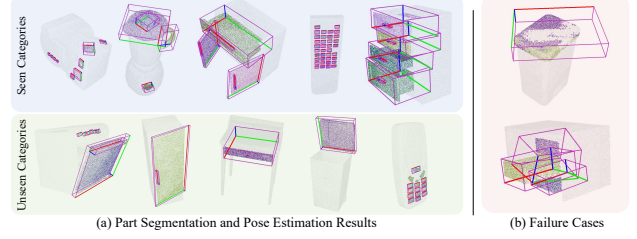


Figure 5. **Qualitative Results.** Left two figures show visualization of cross-category part segmentation and pose estimation on seen and unseen categories, the right shows several failed cases.

category level pose definition, we can design effective interaction policy based on part instance segmentation and pose estimation results.

We can estimate the 6D pose of the part we want to interact with using the method described above. Because our pose definition includes motion information, we can use a simple and efficient heuristic algorithm to interact with it. Furthermore, we created interaction experiments on both simulators and real machines to demonstrate that our algorithm is effective and that our entire project is meaningful to downstream tasks. Please check the appendix for detailed interaction policy for all part classes.

## 6. Experiments

### 6.1. Data Preparation

With our dataset described in Section 3, we render RGB-D images of objects using the SAPIEN environment [53] and generate partial colored point cloud observations. When generating training and testing data, we randomly select camera view points within reasonable perspectives, and set the articulation of the objects to random states.

### 6.2. Cross-Category Part Segmentation

**Evaluation Metrics.** Following the previous 3D semantic instance segmentation benchmarks in ScanNet v2 [7] and S3DIS [1], we use the widely-adopted metric average precision (AP) and AP with IoU threshold 50% (AP50) in 3D to evaluate the performance of part segmentation. We use AP50 (AP with IoU threshold 50%) as the main metric, evaluating the performance on each part class and the overall performance. We also report AP (averages over IoU thresholds from 50% to 95%, with a step of 5%).

**Main Results.** Table 2 shows the quantitative comparisons between our method and previous state-of-the-art methods of 3D instance segmentation.

In both seen and unseen object categories, our method shows significant improvement compared to other methods. For AP50, our method achieves 76.5% in seen categories, which beats the second-runner by 7.7%. In unseen categories, our method achieves 37.2%, significantly higher and

		Ln.F.Hl.	Rd.F.Hl.	Hg.Hl.	Hg.Ld.	Sd.Ld.	Sd.Bn	Sd.Dw.	Hg.Dr.	Hg.Kb.	Avg. AP	Avg. AP50
Seen	PG [18]	86.1	23.0	84.6	80.01	88.3	49.3	62.6	92.8	34.6	57.3	66.8
	SG [42]	57.8	<b>93.6</b>	81.2	76.0	89.3	25.2	50.8	93.9	51.5	58.5	68.8
	Ours	<b>89.2</b>	54.9	<b>90.4</b>	<b>84.8</b>	<b>89.8</b>	<b>66.7</b>	<b>67.2</b>	<b>94.7</b>	<b>52.9</b>	<b>67.6</b>	<b>76.5</b>
Unseen	PG [18]	32.44	9.8	2.1	26.8	0.0	42.6	57.0	63.9	1.7	21.9	26.3
	SG [42]	25.8	5.0	0.4	33.9	0.6	<b>51.5</b>	51.2	69.0	12.1	22.0	27.7
	Ours	<b>45.6</b>	<b>40.0</b>	<b>3.1</b>	<b>40.2</b>	<b>5.0</b>	49.1	<b>64.2</b>	<b>69.1</b>	<b>23.4</b>	<b>32.0</b>	<b>37.2</b>

Table 2. **Results of Part Segmentation on Seen Object Categories and Unseen Object Categories in terms of Per-part-class AP50, Average AP50, and Average AP.** Ln.=Line. F.=Fixed. Rd.=Round. Hl.=Handle. Ld.=Lid. Bn.=Button. Dw.=Drawer. Dr.=Door. Kb.=Knob. PG=PointGroup [18]. SG=SoftGroup [42].

				Seen		Unseen	
use adv	use P-adv	use M-adv	use D-adv	Avg. AP	Avg. AP50	Avg. AP	Avg. AP50
✗				58.8	71.0	22.0	28.0
✓				61.0	70.6	23.2	29.8
✓	✓			62.8	71.6	27.1	32.3
✓	✓	✓		64.9	73.7	29.6	35.0
✓	✓	✓	✓	<b>67.6</b>	<b>76.5</b>	<b>32.0</b>	<b>37.2</b>

Table 3. **Ablation Studies for Domain-generalizable Part Segmentation.** The left four columns stand for using adversarial learning method, using part-oriented feature query technique, using multi-resolution adversarial training and distribution-balancing training technique respectively.

		$R_e \downarrow$	$T_e \downarrow$	$S_e \downarrow$	$\theta_e \downarrow$	$d_e \downarrow$	$mIoU \uparrow$	$A_5 \uparrow$	$A_{10} \uparrow$
Seen	PG [18]	14.3	0.034	0.039	7.947	0.020	49.4	41.2	66.4
	Ours	<b>8.8</b>	<b>0.028</b>	<b>0.035</b>	<b>7.4</b>	<b>0.014</b>	<b>52.2</b>	<b>45.6</b>	<b>71.5</b>
Unseen	PG [18]	18.2	0.056	0.073	12.0	0.031	36.2	28.0	50.9
	Ours	<b>14.8</b>	<b>0.051</b>	<b>0.067</b>	<b>11.3</b>	<b>0.024</b>	<b>43.1</b>	<b>32.0</b>	<b>55.7</b>

Table 4. **Results of Part Pose Estimation on Seen Object Categories and Unseen Object Categories.** PG=baseline modified from PointGroup [18].

relatively 9.5% better than the second-runner. It shows that our method could achieve much better results than previous methods, with especially remarkable generalizability to unseen categories.

**Ablation Studies.** We conduct ablation experiments to demonstrate the usefulness of our domain adversarial learning method as well as our techniques in our domain-generalizable model. We have set up sufficient comparative experiments to demonstrate that our methods and techniques contribute significantly to the generalization ability for seen and unseen object categories as shown in Table 3. By comparing row 1, 2, we can see the domain adversarial training in the object global feature helps the generalization ability to unseen categories, but somewhat at the expense of performance in the seen domain. When introduced our part-oriented adversarial technique(row 2,3), the performance improved no matter on seen or unseen categories. The multi-resolution technique also contributes to the performance in the two areas(row 3,4). The distribution-

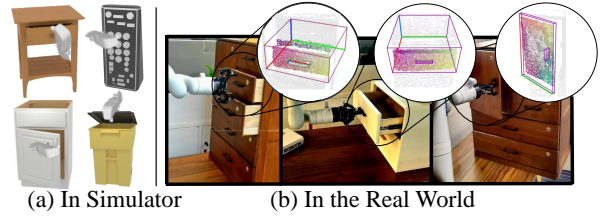


Figure 6. **Cross-category Part-based Object Manipulation.** Left: in simulator, right: in the real world.

balancing techniques(row 4,5) takes the performance of the model a step further and achieves strong accuracy and generalization ability.

### 6.3. Cross-Category Part Pose Estimation

**Evaluation Metrics.** We use the following metrics for cross-category part pose estimation:  $R_e(^{\circ})$ , average rotation error;  $T_e(\text{cm})$ , average translation error;  $S_e$ , average scale error;  $\theta_e(^{\circ})$  rotation error for part interaction axis;  $d_e(\text{cm})$  translation error for part interaction axis; **3D mIoU (mIoU)(%)**, the average 3D intersection over union of ground-truth and predicted bounding boxes; **5°5cm accuracy ( $A_5$ )(%)**, the percentage of pose predictions with rotation error  $< 5^{\circ}$  and translation error  $< 5\text{cm}$ ; **10°10cm accuracy ( $A_{10}$ )(%)**, the percentage of pose predictions with rotation error  $< 10^{\circ}$  and translation error  $< 10\text{cm}$ . And we evaluate part pose only when the part is detected.

**Main Results.** We conduct experiments on Part Pose Estimation task and modify PointGroup [18] as baseline: we adopt PointGroup as backbone and to regress the NPCS value of each points followed by pose fitting. Table 4 shows the quantitative results of our method and the baseline. Our method outperforms baseline method on most of the metrics in seen categories, and on all of the metrics in unseen categories, which shows the value of our domain-invariant feature extraction. With our domain adversarial method and the techniques introduced, the performance of our pose estimation improves a lot, especially in unseen categories.



## 6.4. Cross-Category Part-based Object Manipulation

We showcase the usefulness of part pose by performing cross-category part-based object manipulation on four basic tasks. We use SAPIEN [53] environment for simulation and we set up four experiments based on SAPIEN Manipulation Skill Benchmark [33], (*i.e.* opening drawers, opening doors, using handles, pressing buttons).

**Task Settings.** In this task, a gripper is used for finishing the tasks on the seen or unseen categories. This task exemplifies robot manipulation under the motion constraint of a prismatic or a revolute joint. A success in manipulating objects is defined as opening up part for 90% of the motion range within 1,000 and coming to a stable stop at the end. Please see the appendix for details of the environment setting.

**Heuristics Design and Experiment in Simulator.** We first do cross-category part segmentation and pose estimation using our perception method. Once we have the prediction of the part poses, we move the robot arm toward the parts we want to manipulate, turning the gripper in the direction suitable for grabbing, and then closing the gripper. Finally, we move the gripper along the proposed trajectories toward the target position, following our part pose definition. The results show that our perception model and manipulation heuristics work well, achieve good performance on these tasks, and can generalize to objects from unseen object categories. For more details about our manipulation benchmark setting and experiment results, please refer to the appendix.

**Real Experiment.** Although trained on simulated data, our method can be used in real experiments. We use our method on real objects, and it successfully produces part segmentation and pose prediction. We then use KINOVA robot arm with motion planning and the end effector trajectory, just like what we did in the simulator, and successfully open real drawers and real doors. Please see the appendix for detailed experiments.

## 7. Conclusion

In this work, we reason that learning about generalizable and actionable parts is the key to an intelligent agent capable of cross-category object perception and manipulation. We introduce the definition of GAParts and present GAPartNet dataset by annotating cross-category part classes and part poses. We then do domain-generalizable part segmentation, part pose estimation, and downstream part-based object manipulation. We propose a novel method from the perspective of domain generalization that outperforms previous works on these tasks, and design part-based interaction policies for effective and generalizable robot manipulation in simulation and in real, thanks to our GAPart definition and

our cross-category domain-generalizable perception model.

**Limitations.** The cross-category tasks are challenging, and further research is still needed for better generalizability. For object manipulation, our heuristics method is dependent on precise part pose prediction. Future works may make effort to achieve manipulation results that are more robust to perception errors.

## References

- [1] Iro Armeni, Ozan Sener, Amir R. Zamir, Helen Jiang, Ioannis Brilakis, Martin Fischer, and Silvio Savarese. 3d semantic parsing of large-scale indoor spaces. In *Proceedings of the IEEE International Conference on Computer Vision and Pattern Recognition*, 2016. 7
- [2] Michel Breyer, Jen Jen Chung, Lionel Ott, Siegwart Roland, and Nieto Juan. Volumetric grasping network: Real-time 6 dof grasp detection in clutter. In *Conference on Robot Learning*, 2020. 3
- [3] Angel X Chang, Thomas Funkhouser, Leonidas Guibas, Pat Hanrahan, Qixing Huang, Zimo Li, Silvio Savarese, Manolis Savva, Shuran Song, Hao Su, et al. Shapenet: An information-rich 3d model repository. *arXiv preprint arXiv:1512.03012*, 2015. 3
- [4] Dengsheng Chen, Jun Li, Zheng Wang, and Kai Xu. Learning canonical shape space for category-level 6d object pose and size estimation. In *Proceedings of the IEEE/CVF Conference on Computer Vision and Pattern Recognition (CVPR)*, June 2020. 1, 3
- [5] Shaoyu Chen, Jiemin Fang, Qian Zhang, Wenyu Liu, and Xinggang Wang. Hierarchical aggregation for 3d instance segmentation. In *Proceedings of the IEEE/CVF International Conference on Computer Vision*, pages 15467–15476, 2021. 1
- [6] Wei Chen, Xi Jia, Hyung Jin Chang, Jinming Duan, Linlin Shen, and Ales Leonardis. Fs-net: Fast shape-based network for category-level 6d object pose estimation with decoupled rotation mechanism. In *Proceedings of the IEEE/CVF Conference on Computer Vision and Pattern Recognition (CVPR)*, pages 1581–1590, June 2021. 3
- [7] Angela Dai, Angel X. Chang, Manolis Savva, Maciej Halber, Thomas Funkhouser, and Matthias Nießner. Scannet: Richly-annotated 3d reconstructions of indoor scenes. In *Proc. Computer Vision and Pattern Recognition (CVPR)*, IEEE, 2017. 7
- [8] Hao-Shu Fang, Chenxi Wang, Minghao Gou, and Cewu Lu. Graspnet-1billion: A large-scale benchmark for general object grasping. In *Proceedings of the IEEE/CVF conference on computer vision and pattern recognition*, pages 11444–11453, 2020. 3
- [9] Martin A Fischler and Robert C Bolles. Random sample consensus: a paradigm for model fitting with applications to image analysis and automated cartography. *Communications of the ACM*, 24(6):381–395, 1981. 7
- [10] Samir Yitzhak Gadre, Kiana Ehsani, and Shuran Song. Act the part: Learning interaction strategies for articulated object

- part discovery. In *Proceedings of the IEEE/CVF International Conference on Computer Vision*, pages 15752–15761, 2021. 3
- [11] Yaroslav Ganin and Victor Lempitsky. Unsupervised domain adaptation by backpropagation. In *International conference on machine learning*, pages 1180–1189. PMLR, 2015. 2, 3, 6
- [12] Yaroslav Ganin, Evgeniya Ustinova, Hana Ajakan, Pascal Germain, Hugo Larochelle, François Laviolette, Mario Marchand, and Victor Lempitsky. Domain-adversarial training of neural networks. *The journal of machine learning research*, 17(1):2096–2030, 2016. 2, 3, 6
- [13] Benjamin Graham and Laurens van der Maaten. Submanifold sparse convolutional networks. *arXiv preprint arXiv:1706.01307*, 2017. 5
- [14] Kaiming He, Georgia Gkioxari, Piotr Dollár, and Ross Girshick. Mask r-cnn. In *Proceedings of the IEEE international conference on computer vision*, pages 2961–2969, 2017. 1, 13
- [15] Kaiming He, Xiangyu Zhang, Shaoqing Ren, and Jian Sun. Deep residual learning for image recognition. *arXiv preprint arXiv:1512.03385*, 2015. 13
- [16] Yisheng He, Haibin Huang, Haoqiang Fan, Qifeng Chen, and Jian Sun. Ffb6d: A full flow bidirectional fusion network for 6d pose estimation. In *Proceedings of the IEEE/CVF Conference on Computer Vision and Pattern Recognition (CVPR)*, pages 3003–3013, June 2021. 3
- [17] Junguang Jiang, Baixu Chen, Jianmin Wang, and Mingsheng Long. Decoupled adaptation for cross-domain object detection. *arXiv preprint arXiv:2110.02578*, 2021. 3
- [18] Li Jiang, Hengshuang Zhao, Shaoshuai Shi, Shu Liu, Chi-Wing Fu, and Jiaya Jia. Pointgroup: Dual-set point grouping for 3d instance segmentation. In *Proceedings of the IEEE/CVF Conference on Computer Vision and Pattern Recognition*, pages 4867–4876, 2020. 1, 5, 8, 12, 13
- [19] Zhenyu Jiang, Yifeng Zhu, Maxwell Svetlik, Kuan Fang, and Yuke Zhu. Synergies between affordance and geometry: 6-dof grasp detection via implicit representations. *Robotics: science and systems*, 2021. 3
- [20] Alexander Kirillov, Yuxin Wu, Kaiming He, and Ross Girshick. Pointrend: Image segmentation as rendering. In *Proceedings of the IEEE/CVF conference on computer vision and pattern recognition*, pages 9799–9808, 2020. 1
- [21] Yann Labbé, Justin Carpentier, Mathieu Aubry, and Josef Sivic. Cosypose: Consistent multi-view multi-object 6d pose estimation. In *European Conference on Computer Vision*, pages 574–591. Springer, 2020. 3
- [22] Haoliang Li, Sinno Jialin Pan, Shiqi Wang, and Alex C Kot. Domain generalization with adversarial feature learning. In *Proceedings of the IEEE conference on computer vision and pattern recognition*, pages 5400–5409, 2018. 2, 3, 6
- [23] Jue Kun Li, Wee Sun Lee, and David Hsu. Push-net: Deep planar pushing for objects with unknown physical properties. In *Robotics: Science and Systems*, volume 14, pages 1–9, 2018. 3
- [24] Xiaolong Li, He Wang, Li Yi, Leonidas Guibas, A Lynn Abbott, and Shuran Song. Category-level articulated object pose estimation. *Proceedings of the IEEE Conference on Computer Vision and Pattern Recognition*, 2020. 1, 2, 4, 7
- [25] Yangyan Li, Rui Bu, Mingchao Sun, Wei Wu, Xinhan Di, and Baoquan Chen. Pointcnn: Convolution on x-transformed points. *NeurIPS*, 2018. 3
- [26] Yi Li, Gu Wang, Xiangyang Ji, Yu Xiang, and Dieter Fox. Deepim: Deep iterative matching for 6d pose estimation. In *Proceedings of the European Conference on Computer Vision (ECCV)*, pages 683–698, 2018. 3
- [27] Liu Liu, Wenqiang Xu, Haoyuan Fu, Sucheng Qian, Qiaojun Yu, Yang Han, and Cewu Lu. Akb-48: A real-world articulated object knowledge base. In *Proceedings of the IEEE/CVF Conference on Computer Vision and Pattern Recognition*, pages 14809–14818, 2022. 2, 4, 5, 12
- [28] Xueyi Liu, Xiaomeng Xu, Anyi Rao, Chuang Gan, and Li Yi. Autogpart: Intermediate supervision search for generalizable 3d part segmentation. In *Proceedings of the IEEE/CVF Conference on Computer Vision and Pattern Recognition*, pages 11624–11634, 2022. 3
- [29] Tiange Luo, Kaichun Mo, Zhiao Huang, Jiarui Xu, Siyu Hu, Liwei Wang, and Hao Su. Learning to group: A bottom-up framework for 3d part discovery in unseen categories. *arXiv preprint arXiv:2002.06478*, 2020. 3
- [30] Kaichun Mo, Paul Guerrero, Li Yi, Hao Su, Peter Wonka, Niloy Mitra, and Leonidas J Guibas. Structurennet: Hierarchical graph networks for 3d shape generation. *arXiv preprint arXiv:1908.00575*, 2019. 3
- [31] Kaichun Mo, Leonidas J Guibas, Mustafa Mukadam, Abhinav Gupta, and Shubham Tulsiani. Where2act: From pixels to actions for articulated 3d objects. In *Proceedings of the IEEE/CVF International Conference on Computer Vision*, pages 6813–6823, 2021. 3
- [32] Kaichun Mo, Shilin Zhu, Angel X Chang, Li Yi, Subarna Tripathi, Leonidas J Guibas, and Hao Su. Partnet: A large-scale benchmark for fine-grained and hierarchical part-level 3d object understanding. In *CVPR*, 2019. 2, 3
- [33] Tongzhou Mu, Zhan Ling, Fanbo Xiang, Derek Yang, Xuanlin Li, Stone Tao, Zhiao Huang, Zhiwei Jia, and Hao Su. ManiSkill: Generalizable Manipulation Skill Benchmark with Large-Scale Demonstrations. In *Annual Conference on Neural Information Processing Systems (NeurIPS)*, 2021. 2, 3, 9, 14
- [34] Despoina Paschalidou, Angelos Katharopoulos, Andreas Geiger, and Sanja Fidler. Neural parts: Learning expressive 3d shape abstractions with invertible neural networks. In *Proceedings of the IEEE/CVF Conference on Computer Vision and Pattern Recognition*, pages 3204–3215, 2021. 3
- [35] Sida Peng, Yuan Liu, Qixing Huang, Xiaowei Zhou, and Hujun Bao. Pvnnet: Pixel-wise voting network for 6dof pose estimation. In *Proceedings of the IEEE/CVF Conference on Computer Vision and Pattern Recognition*, pages 4561–4570, 2019. 3
- [36] Charles R Qi, Hao Su, Kaichun Mo, and Leonidas J Guibas. Pointnet: Deep learning on point sets for 3d classification and segmentation. In *CVPR*, pages 652–660, 2017. 3
- [37] Charles Ruizhongtai Qi, Li Yi, Hao Su, and Leonidas J Guibas. Pointnet++: Deep hierarchical feature learning on point sets in a metric space. *NeurIPS*, 2017. 3

- [38] Shaoqing Ren, Kaiming He, Ross Girshick, and Jian Sun. Faster r-cnn: Towards real-time object detection with region proposal networks. *Advances in neural information processing systems*, 28, 2015. 1
- [39] Martin Sundermeyer, Zoltan-Csaba Marton, Maximilian Durner, Manuel Brucker, and Rudolph Triebel. Implicit 3d orientation learning for 6d object detection from rgb images. In *Proceedings of the european conference on computer vision (ECCV)*, pages 699–715, 2018. 3
- [40] Meng Tian, Marcelo H Ang Jr, and Gim Hee Lee. Shape prior deformation for categorical 6d object pose and size estimation. In *Proceedings of the European Conference on Computer Vision (ECCV)*, August 2020. 3
- [41] Shinji Umeyama. Least-squares estimation of transformation parameters between two point patterns. *IEEE Transactions on Pattern Analysis & Machine Intelligence*, 13(04):376–380, 1991. 7
- [42] Thang Vu, Kookhoi Kim, Tung M Luu, Thanh Nguyen, and Chang D Yoo. Softgroup for 3d instance segmentation on point clouds. In *Proceedings of the IEEE/CVF Conference on Computer Vision and Pattern Recognition*, pages 2708–2717, 2022. 5, 8
- [43] Chen Wang, Roberto Martín-Martín, Danfei Xu, Jun Lv, Cewu Lu, Li Fei-Fei, Silvio Savarese, and Yuke Zhu. 6-pack: Category-level 6d pose tracker with anchor-based keypoints. In *2020 IEEE International Conference on Robotics and Automation (ICRA)*, pages 10059–10066. IEEE, 2020. 3
- [44] Chen Wang, Danfei Xu, Yuke Zhu, Roberto Martín-Martín, Cewu Lu, Li Fei-Fei, and Silvio Savarese. Densefusion: 6d object pose estimation by iterative dense fusion. In *Proceedings of the IEEE/CVF conference on computer vision and pattern recognition*, pages 3343–3352, 2019. 3
- [45] He Wang, Srinath Sridhar, Jingwei Huang, Julien Valentin, Shuran Song, and Leonidas J Guibas. Normalized object coordinate space for category-level 6d object pose and size estimation. In *CVPR*, pages 2642–2651, 2019. 1, 3, 4
- [46] Jiaze Wang, Kai Chen, and Qi Dou. Category-level 6d object pose estimation via cascaded relation and recurrent reconstruction networks. In *2021 IEEE/RSJ International Conference on Intelligent Robots and Systems (IROS)*, pages 4807–4814. IEEE, 2021. 3
- [47] Jindong Wang, Cuiling Lan, Chang Liu, Yidong Ouyang, Tao Qin, Wang Lu, Yiqiang Chen, Wenjun Zeng, and Philip Yu. Generalizing to unseen domains: A survey on domain generalization. *IEEE Transactions on Knowledge and Data Engineering*, pages 1–1, 2022. 3
- [48] Weiye Wang, Ronald Yu, Qiangui Huang, and Ulrich Neumann. Sgpn: Similarity group proposal network for 3d point cloud instance segmentation. In *Proceedings of the IEEE conference on computer vision and pattern recognition*, pages 2569–2578, 2018. 3
- [49] Xiaogang Wang, Bin Zhou, Yahao Shi, Xiaowu Chen, Qinpeng Zhao, and Kai Xu. Shape2motion: Joint analysis of motion parts and attributes from 3d shapes. In *Proceedings of the IEEE/CVF Conference on Computer Vision and Pattern Recognition*, pages 8876–8884, 2019. 2
- [50] Yue Wang, Yongbin Sun, Ziwei Liu, Sanjay E Sarma, Michael M Bronstein, and Justin M Solomon. Dynamic graph cnn for learning on point clouds. *ACM TOG*, 38(5):1–12, 2019. 3
- [51] Yijia Weng, He Wang, Qiang Zhou, Yuzhe Qin, Yueqi Duan, Qingnan Fan, Baoquan Chen, Hao Su, and Leonidas J Guibas. Captra: Category-level pose tracking for rigid and articulated objects from point clouds. In *Proceedings of the IEEE/CVF International Conference on Computer Vision*, pages 13209–13218, 2021. 1, 3
- [52] Ruihai Wu, Yan Zhao, Kaichun Mo, Zizheng Guo, Yian Wang, Tianhao Wu, Qingnan Fan, Xuelin Chen, Leonidas Guibas, and Hao Dong. VAT-mart: Learning visual action trajectory proposals for manipulating 3d ARTiculated objects. In *International Conference on Learning Representations*, 2022. 3
- [53] Fanbo Xiang, Yuzhe Qin, Kaichun Mo, Yikuan Xia, Hao Zhu, Fangchen Liu, Minghua Liu, Hanxiao Jiang, Yifu Yuan, He Wang, et al. Sapien: A simulated part-based interactive environment. In *CVPR*, 2020. 2, 4, 5, 7, 9, 12, 14
- [54] Yu Xiang, Tanner Schmidt, Venkatraman Narayanan, and Dieter Fox. Posecnn: A convolutional neural network for 6d object pose estimation in cluttered scenes. In *Robotics: Science and Systems (RSS)*, 2018. 3
- [55] Chao Xu, Yixin Chen, He Wang, Song-Chun Zhu, Yixin Zhu, and Siyuan Huang. Partafford: Part-level affordance discovery from 3d objects. *arXiv preprint arXiv:2202.13519*, 2022. 3
- [56] Kaizhi Yang and Xuejin Chen. Unsupervised learning for cuboid shape abstraction via joint segmentation from point clouds. *ACM Transactions on Graphics (TOG)*, 40(4):1–11, 2021. 3
- [57] Li Yi, Vladimir G Kim, Duygu Ceylan, I-Chao Shen, Mengyan Yan, Hao Su, Cewu Lu, Qixing Huang, Alla Sheffer, and Leonidas Guibas. A scalable active framework for region annotation in 3d shape collections. *ACM TOG*, 35(6):1–12, 2016. 2, 3
- [58] Li Yi, Wang Zhao, He Wang, Minhyuk Sung, and Leonidas J Guibas. Gspn: Generative shape proposal network for 3d instance segmentation in point cloud. In *Proceedings of the IEEE/CVF Conference on Computer Vision and Pattern Recognition*, pages 3947–3956, 2019. 3
- [59] Fenggen Yu, Kun Liu, Yan Zhang, Chenyang Zhu, and Kai Xu. Partnet: A recursive part decomposition network for fine-grained and hierarchical shape segmentation. In *Proceedings of the IEEE/CVF Conference on Computer Vision and Pattern Recognition*, pages 9491–9500, 2019. 2
- [60] Kuan-Ting Yu, Maria Bauza, Nima Fazeli, and Alberto Rodriguez. More than a million ways to be pushed. In *2016 IEEE/RSJ international conference on intelligent robots and systems (IROS)*, pages 30–37. IEEE, 2016. 3

## A. More Details of GAPartNet dataset

In this section, we first introduce more details of our definition of GAParts, including semantics and pose. Then we explain the challenges we meet to annotate the dataset and our solution. More visualization of example objects of each GAPart class is provided as well.

### A.1. More Details of GAPart Definition

**GAPart Semantics.** Based on the geometric similarity and actionability alignment, 9 common GAPart classes are defined in our work: *line fixed handle*, *round fixed handle*, *hinge handle*, *hinge lid*, *slider lid*, *slider button*, *slider drawer*, *hinge door*, *hinge knob*. Note that actionability is explicitly encoded in the class names, *slider*, *hinge*, *fixed*, with *slider* suggesting translation, *hinge* suggesting rotation, and *fixed* suggesting a fixed attachment where the two different parts can not move separately.

**GAPart Poses.** For GAParts, the definition of the canonicalized part orientation in NPCS is rooted in *interaction*. Specifically, we consistently specify the approaching direction in the definition, based on the observation that the interaction policy for parts is mainly determined by the approaching direction. We define the z-axis as the direction pointing out from the approaching direction of such parts. For example, we move reversely along the z-axis to grab a round fixed handle, press a slider button, or place a slider lid back on its container body. Additionally, the approaching direction is perpendicular to the surface of hinge doors and hinge lids, in which they open and close.

For each GAPart class, we define its specific symmetry pattern by considering its geometry and actionability. We allow any rotation around the z-axis for hinge knobs, slider lids, round fixed handles, and slider buttons. We allow a 180°-flip around the z-axis for line fixed handles and hinge handles that do not have rotational symmetry around the z-axis. Note that for hinge lids and hinge doors, the right-hand rule is followed when considering their poses, so no symmetry will exist. And for slider drawers, the canonicalized part orientation is well-defined in NPCS, so no symmetry will exist as well.

### A.2. More Details of Data Annotation

GAPartNet dataset is constructed based on two existing datasets, PartNet-Mobility [53] and AKB-48 [27]. Focusing on the GAParts we define, we select 23 object categories from PartNet-Mobility [53] and 4 object categories from AKB-48 [27].

Most of the 3D object shapes of GAPartNet are from PartNet-Mobility [53]. Since the texture of shapes in PartNet-Mobility [53] is all synthetic, to mitigate the Sim2Real gap, we further leverage the shapes from AKB-48 [27] whose texture is scanned from the real world.

However, the original PartNet-Mobility [53] and AKB-48 [27] lack of directly usable information we need to do our new annotation. First, they do not provide directly usable consistent semantic annotations to similar parts across object categories. For example, some handles on *Door* are labeled as *door*, while some doors on *StorageFurniture* are labeled as *frame*. Secondly, their original annotation is not as fine-grained as we need. Specifically, fixed han-

dles, *i.e.* line fixed handles and round fixed handles, are not annotated as individual parts, since they are attached to either base bodies or other movable parts. Their meshes are merged with others which leaves rare semantic cues to re-separate them. Finally, there are a lot of meshes of parts that we care about are imperfect, which seriously limits either the quality of our pose annotation or the quality of rendered images.

To address these issues, we first manually go over all objects to re-separate the meshes of fixed handles from the original 3D object shapes. We also modify the kinematic chains to re-merge these meshes into new links and add corresponding fixed joints, which provides more consistent annotation and is beneficial for following robotic tasks. In this step, more than 1000 fixed handles are re-separated and re-merged. Secondly, we go over all 1166 objects in GAPartNet and clean all original semantic annotations to align with our GAPart class definition. Thirdly, we manually use MeshLab and some heuristics to modify all imperfect meshes, not only cutting the redundant meshes off but also fixing the one-sided meshes. More than 100 object instances are modified.

Finally, with the 1166 3D object shapes with new semantic annotation and modified meshes, we use a lot of heuristics to fit the oriented tight bounding boxes of all 8489 GAParts, corresponding to their canonical orientations, and add our annotations. With our effort, GAPartNet is capable of detection, segmentation, pose estimation, and manipulation on cross-category generalizable and actionable parts.

### A.3. More Visualization of GAPartNet

Example objects of each GAPart class from seen categories and unseen categories are shown in Figure 7.

## B. More Details of Part Segmentation

In this section, we provide the implementation details for the part instance segmentation task. We first include details of our network, and then introduce our training procedure.

### B.1. Network Architecture

In mask proposal extraction stage, we use the same structure as PointGroup [18]. We set the cluster radius to 0.03 and cluster point number threshold to 5 to get good segmentation results in GAPartNet dataset.

In scoring stage, we first voxelize the input 20,000-point point cloud ( $N = 20,000$ ) into a  $100 \times 100 \times 100$  voxel grid. The backbone U-Net has a depth of 6 and outputs a  $N \times K$  per-point feature  $\mathbf{F}$  where  $K = 16$ . Then, each mask proposal  $C_i$  is normalized and voxelized again into a  $50 \times 50 \times 50$  voxel grid and we use a 1-depth U-Net based on sparse convolution to extract per-point feature in



the shape of  $N_i \times 16$ , where  $N_i$  is the number of points in  $C_i$ . At last, we do ROI Pooling with the feature of foreground points to get the per-mask feature, followed by a linear layer to extract the final per-mask score  $S$ . At test time, points with binary classification scores below 0.4 will be filtered out as background, and we discard the masks with less than 5 points or with a score lower than 0.09. Finally, Non-Maximum Suppression (NMS) with IoU threshold 0.3 is applied to get the final masks.

For domain adversarial learning, we introduce Gradient Reverse Layer (GRL) with  $\alpha = 0.3$  for the negative gradient and 3 domain discriminator with the similar architecture as the scoring stage mentioned above with a linear and sigmoid layer for domain classification, placing at the 2-nd, 4-th, 6-th decoder layer of the Sparse Unet backbone.

## B.2. Training Procedure

For mask proposal extraction, we train the 2D detector Mask RCNN [14] and the 3D detector PointGroup [18] on our GPartNet dataset. For the 2D detector, we initialize the network from ResNet50 backbone model pre-trained on ImageNet provided by [15]. We train the network for 150,000 iterations with the SGD optimizer with batch size 12 and an initial learning rate of 0.01. During training, we decay the learning rate at 60,000 iterations and 100,000 iterations, with  $\times 0.1$  each time. This training process takes around 8 hours on four Nvidia GeForce RTX 2080 Ti GPUs. For the 3D detector, we train the network from scratch for 368 epochs, with prepare-epochs set to 128 epochs. We use the Adam optimizer with batch size 48 and an initial learning rate of 0.001. This training process takes around 8 days on a single Nvidia GeForce RTX 2080 Ti GPU.

For mask proposal scoring and adversarial training, we use the Adam optimizer with batch size 32 and an initial learning rate of 0.001. The learning rate is decayed with  $\times 0.1$  for every 100 epochs. This training process takes around 70 hours on a single Nvidia GeForce RTX 2080 Ti GPU. Then we train the whole network including feature extraction, domain classification and scoring, for 64 epochs. We use the Adam optimizer with batch size 32 and the initial learning rate of 0.001. This training process takes around 10 hours on a single Nvidia GeForce RTX 2080 Ti GPU.

## C. More Details of Part Pose Estimation

### C.1. Network Architecture

In NPCS prediction stage, we use the predicted part segmentation masks as input. Similar to the previous stage, we normalize and voxelize each mask proposal  $C_i$  into a  $50 \times 50 \times 50$  voxel grid. We use a 1-depth U-Net based on sparse convolution to extract per-point feature in the shape of  $N_i \times 16$ , where  $N_i$  is the number of points in  $C_i$ . Then

three  $16 \times 9$  linear layers with sigmoid are used to predict NPCS coordinates in 9 channels. And We only supervise the channel corresponding to the semantic label.

### C.2. Training Procedure

In NPCS prediction stage, we use the segmentation model from the previous stage as backbone and train the NPCS prediction network for 100 epochs. We use the Adam optimizer with batch size 64 and an initial learning rate of 0.001. The learning rate is decayed with  $\times 0.1$  for every 100 epochs. This training process takes around 60 hours on a single Nvidia GeForce RTX 2080 Ti GPU.

## D. More Details of Part-based Object Manipulation

In this section, we first introduce more details of interaction policy for each part class, and then explain details of experiments in the simulation environment and reality, respectively.

### D.1. Interaction Policy

(1) Round Fixed Handle: For round fixed handles, we use the gripper to approach the handle from the positive direction of the z-axis, and then open the gripper to a width that exceeds the side length of the bounding box, and then close the gripper to complete the grasping.

(2) Line Fixed Handle: The interaction policy for line fixed handles is similar to round fixed handles. Note that we want the opening direction of our gripper and the line fixed handle to be perpendicular, so we turn the opening direction parallel to the y-axis of the predicted bounding box.

(3) Hinge Handle: The interaction policy for hinge handles is similar to line fixed handles. After approaching and grasping the hinge handle, we can rotate it along the predicted axis of the revolute joint.

(4) Slider Button: For slider buttons, we close the gripper and approach the button from the positive direction of the z-axis, and then press the button.

(5) Hinge Knob: For hinge knobs, we clamp the knob like a round handle and rotate the end-effector to complete the task.

(6) Slider Drawer: A gripper approaches an open drawer along the z-axis to fetch something in the drawer, and approaches a drawer against the x-axis to open it. More often than not, we expect to grab a handle hopefully located on the front face of a drawer.

(7) Hinge Door: For hinge doors with handles on the front face, we grab the handle to open the door. After grabbing the handles, the gripper rotates around the predicted shaft of the hinge door to complete the opening or closing of the hinge door. For doors without handles, if the door is not closed, we use the gripper to clamp the outer edge along the y-axis of the bounding box and open the door.

	Drawer		Door		Button		Lid	
	Seen	Unseen	Seen	Unseen	Seen	Unseen	Seen	Unseen
number of evaluation cases	20	20	20	20	20	20	10	10
success cases	19	18	14	11	20	19	7	5

Table 5. **Statistics and Results for Cross-category Object Manipulation in SAPIEN Simulator [53]**

(8) Hinge lid: for hinge lids, we use an interaction method similar to hinge doors.

(9) Slider lid: for slider lids with handles, we grab the handles to open the lids. Otherwise, we use the gripper to clamp the edge of the lid along the x-y-plane of the bounding box, and then move up and down along the z-axis to open and close the lid.

## D.2. Simulation Experiments

**Settings** We set up our interaction environment using SAPIEN [53] simulator, modified from ManiSkill challenge [33]. We randomly pick objects that contain doors, drawers, handles, and lids from unseen instances of the seen categories. We pick such objects that, given the ground truth part segmentation and pose, can be opened successfully using our heuristics. To test the generalizability of our method, our collection of test data comes from different object categories. In this task, a gripper is used for opening a drawer or a door, manipulating a handle, or pressing a button on an unseen object. This task exemplifies robot manipulation under the motion constraint of a prismatic or a revolute joint. Compared to ManiSkill Challenge [33], we limit our observation to a first-frame-only partial point cloud of the object, with a mask indicating which part to interact with. Given the initial state of the robot, our robot performs the whole manipulation based only on the observation at the first time step. The action space of the robot is the motor command of the 6 joints of the robot to determine the pose of the gripper, and we use position control to open or close grippers. A success in opening the drawer, the door or the lid and pressing the button is defined as opening up the part for 90% of the motion range within 1,000 steps with a stable stop at the end. For door, drawer, button manipulation tasks, we use 20 objects from seen categories and 20 from the unseen to construct our benchmarks respectively while for lid categories, the objects from seen and unseen object categories are both 10. The results of the manipulation tasks are shown in the table above.

**Part-pose-based Manipulation Heuristics** We use the interaction policy based on the heuristics mentioned in D.1 to open drawers and doors, manipulate handles, and press buttons. Specifically, when we get the part pose, we can immediately get the grasping pose with our policy. Then we use the motion planning library mplib provided by SAPIEN [53] to move our gripper to the grasping pose. Then with our interaction policy and axis predicted from our method,

we design the end-effector trajectory just along the trajectory of the part moving and interpolate the trajectory with a time step of  $\frac{1}{250}$ . With Inverse Kinematics and PID controller, we solve poses of joints and move the end-effector along the trajectory. All of our implementations are decoupled from ROS and can be implemented in other simulators easily.

## D.3. Real Experiments

In real experiments, we use the KINOVA robot arm with motion planning and the end-effector trajectory just like what we did in the simulator. For manipulation tasks in the real world, a partial point cloud of the target object instance is acquired from the RGB-D camera. With our proposed network and manipulation heuristics, the pose trajectory of the end-effector can be predicted. Then we use the IK algorithm to solve the pose of KINOVA to follow our end-effector trajectory.

*Cross-Category Generalizable and Actionable Parts in GPartNet*

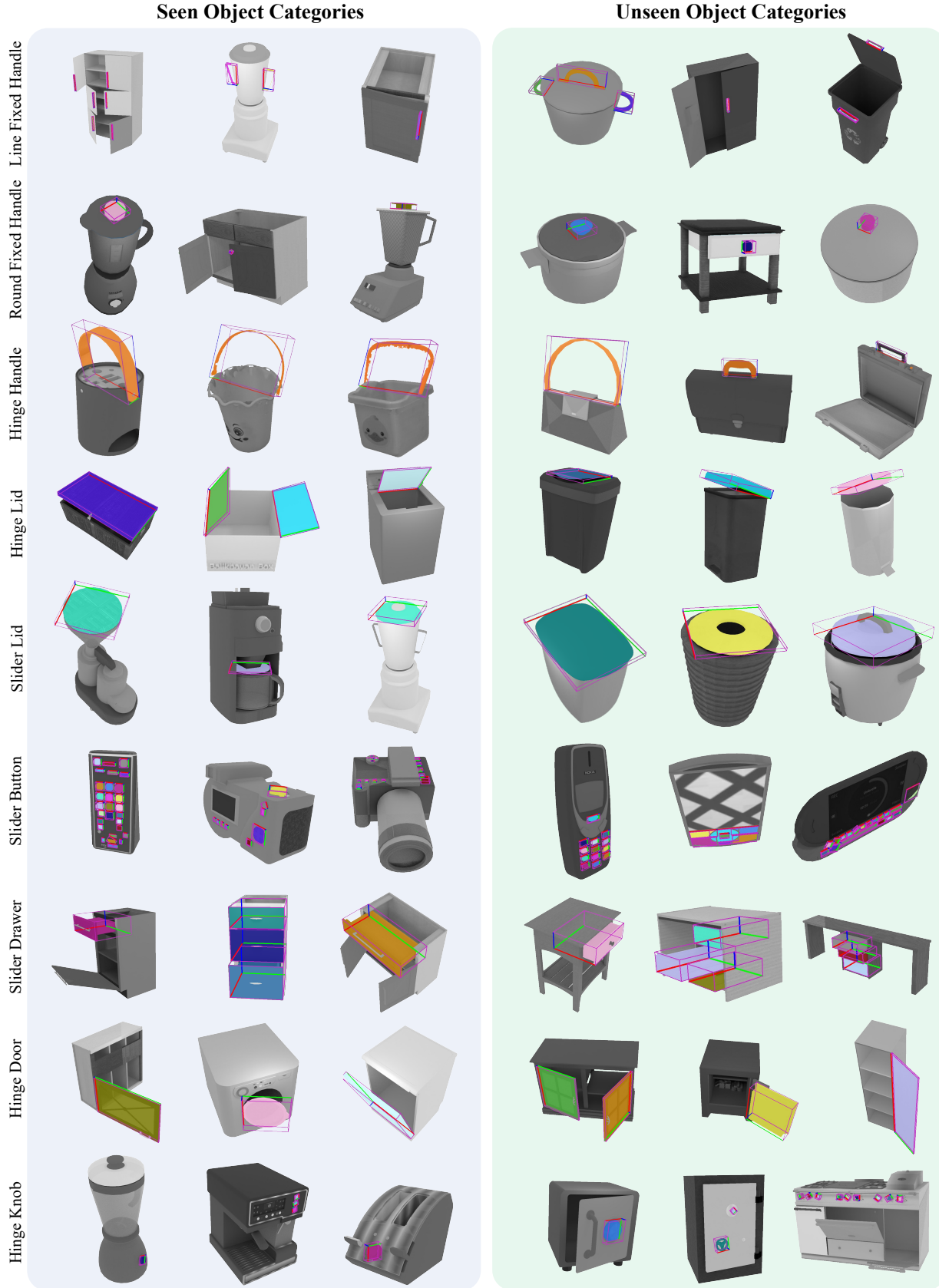


Figure 7. **Example Objects of Each GPart Class from Seen Categories and Unseen Categories.** We show objects in gray scale, GPart segmentation masks in color, and GPart poses using oriented tight bounding boxes.